JOURNAL OF MATERIALS SCIENCE 31 (1996) 6063–6067

Modelling of an electrolyte matrix for a phosphoric acid fuel cell

K. H. YOON, J. H. HUH, J. H. JANG
Department of Ceramic Engineering, Yonsei University, Seoul 120–749, Korea
C. S. KIM
Fuel Cell Research Team, Korea Institute of Energy Research, Taejon 305–343, Korea
E. S. KIM
Department of Materials Engineering, Kyonggi University, Suwon 442–760, Korea

A simple model of an electrolyte matrix for use in a phosphoric acid fuel cell (PAFC) has been proposed. It has important features in the vertical direction. Acid absorbency, bubble pressure and current density as a function of porosity and pore-size distribution were calculated. The calculated values were compared with the real values obtained from a matrix made by rolling and tape casting. The tendency of the properties in the model concurred with the real matrix. Predictions were made for the best performance. The results were a porosity of 80%, a composition having 20% of 0.01–0.1 μm pores and 75% of 0.1–1 μm and 5% of 1–10 μm pores, the thickness of the matrix being 100 μm and the particle size 1.5 μm. It is expected that these theoretical results could be helpful in making a real matrix.

1. Introduction

A fuel cell is a power system that generates electrical energy by an electrochemical reaction in which ionized hydrogen and oxygen produce water. This process has a higher efficiency than that of other heat engines because no energy is dispersed as heat. Fuel cells also produce no environmental pollutants, such as scrap materials or noise. Therefore, it is anticipated that fuel cells will be an important non-polluting power system for the next century [1–3]. Among the various types, a phosphoric acid fuel cell operates at a relatively low working temperature owing to the higher ionic conductivity of liquid phosphoric acid. The practical use of phosphoric acid fuel cells has been investigated [4, 5].

As a device for retaining phosphoric acid, an electrolyte matrix must satisfy many conditions. It must be resistant to corrosion and must be able to retain much phosphoric acid to maintain a high ionic conductivity. It must have a high speed of acid absorbency to prevent decrease of the phosphoric acid concentration by water produced. To fulfil these requirements, the matrix must have a high porosity and an affinity with phosphoric acid. In addition, the electrolyte matrix needs to have a high bubble pressure in order to prevent gas crossover of hydrogen and oxygen [6, 7].

SiC powder with SiC whiskers and polytetrafluoroethylene (PTFE) or polyethersulphone (PES) as a binder are used as the composite materials, and the matrix is formed by rolling or tape casting [8, 9]. Optimization of the conditions for the required properties is very difficult owing to the many factors influencing the matrix properties. To reduce expense and time, a virtual model has been proposed, and detailed calculations for the properties of matrix were compared with experimental results. Through this model the best conditions could be predicted.

2. The model

2.1. Basic model

After preparation of the matrix by rolling and tape casting the SiC powder and SiC whiskers with PES, scanning electron microscopic (SEM) analysis was performed to establish a model, as shown in Fig. 1. The matrix had a porous SiC structure with interconnected pores. Even though porosity and pore size were not uniform in a real matrix, the following points were for simplicity of calculation.

First, the matrix is assumed to be composed of the same size particles, and that there are no differences between the surface and the inner space. Second, the particles are assumed to form pillars by connecting with each other only vertically [10]. This connection is made by the binder. The influence of the shapes of particles and the binder on bubble pressure or current was neglected. Third, the hydrogen ion produced on the electro-catalyst is assumed to move to the opposite electrode only in the vertical direction, so that the ions move the shortest length possible.

This model considered properties only in the vertical direction and neglected the shape effect, because the most important properties in real use (bubble pressure and current density) are the vertical factors, even though the effect of shape can be substituted in

0022–2461 © *1996 Chapman & Hall*

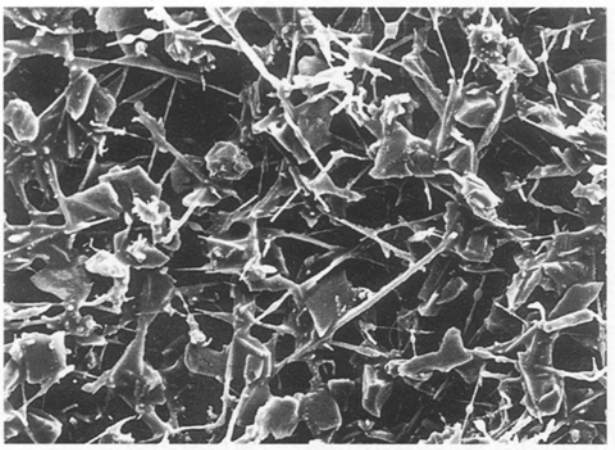

Figure 1 Scanning electron micrograph of the real matrix.

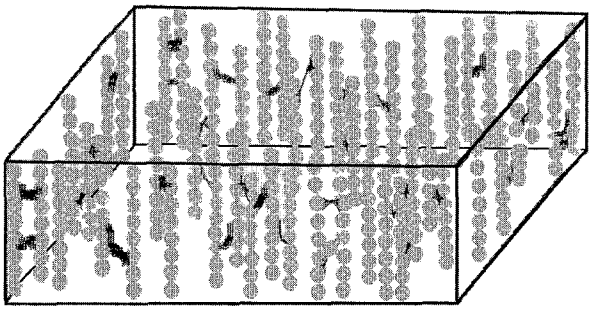

Figure 2 The created model (the grey balls are SiC and the black lines are binder).

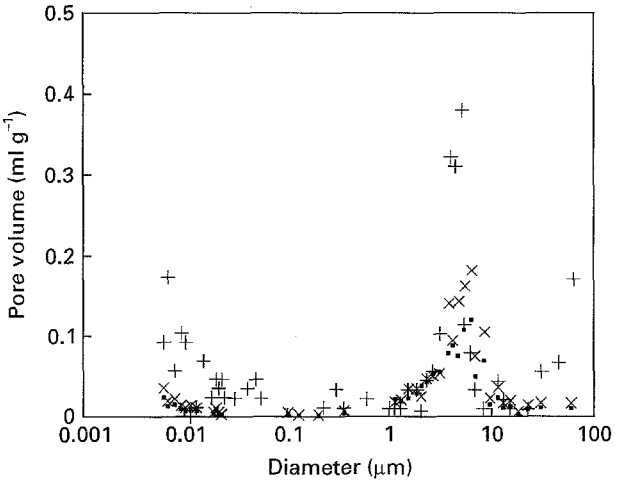

Figure 3 Pore-size distribution of the real matrix, obtained by (+) tape casting with low-viscosity slurry, (×) tape casting with high-viscosity slurry, (■) rolling.

the simulated result by changing the thickness factor. The model created is shown in Fig. 2.

2.2. Extension of the model

The pore-size distributions of a real matrix are shown in Fig. 3 for use in deciding the pore-size distributions that can be made in the model. As shown in Fig. 3, the pores were 0.01–50 μm long, and the distribution could be changed by composition, preparation method, type and quantity of additives. For the modelling of all these cases it was assumed that the porosity and pore-size distribution could be changed freely in the range of 0.01–50 μm. For simplicity of calculation, the pore size was divided into four groups: 0.01–0.1 μm, 0.1–1 μm, 1–10 μm and 10–50 μm. The 0.01–0.1 μm pores were thought to be made not by space between pillars of the matrix composition but by the matrix composition itself or additives like the binder. They were regarded as pores produced by connections of components in this model because the effects of these factors were neglected.

The phosphoric acid could be retained in all pores. In fact, the acid absorbency varied according to retaining speed and retaining method. In this model all pores were assumed to be filled with phosphoric acid with perfect wetting and did not vary with time.

The bubble pressure was calculated using the following equation in the case of having one type of pore [11]

$$P = \frac{2\gamma}{r}\cos\theta \tag{1}$$

where P is the bubble pressure, γ the surface tension of the electrolyte, θ the contact angle, and r the pore radius.

For a matrix having two or more types of pore, the bubble pressure was calculated in the mixed ratio of each part. As the porosity increased, the bubble pressure decreased proportional to the area of pores in the surface of the matrix.

Current density was also calculated on the basis of the above properties. The ions created at the platinum catalyst (experimental data were used for the quantity of ions) were assumed to be conducted by the pores occupying the surface of the matrix. The conduction of the ions is by diffusion, so the conduction was assumed to occur only through the shortest path in the vertical direction and the voltage drop from the polarization in the interface between electrolyte and catalysis was considered [12, 13]. Because the ion- conduction path is affected by the shape of pores and the arrangement of composites in the real matrix, the effect of pore size on the ion-conduction path was considered.

3. Comparison with experiments

The calculated values were compared with experimental values from the matrix made by rolling and tape casting.

Fig. 4 shows a plot of acid absorbency versus porosity. The calculated acid absorbency increased with increase in the porosity, while experimental values were less than calculated values. A possible explanation is that the 0.01–0.1 μm long pores were not retained in the real matrix because it takes a long time for phosphoric acid retention in the matrix. This explanation is supported by the fact that the matrix made by the rolling process does not have this size of pore (as shown in Fig. 3) and had smaller differences between calculated and experimental values than matrices prepared by the tape-casting process.

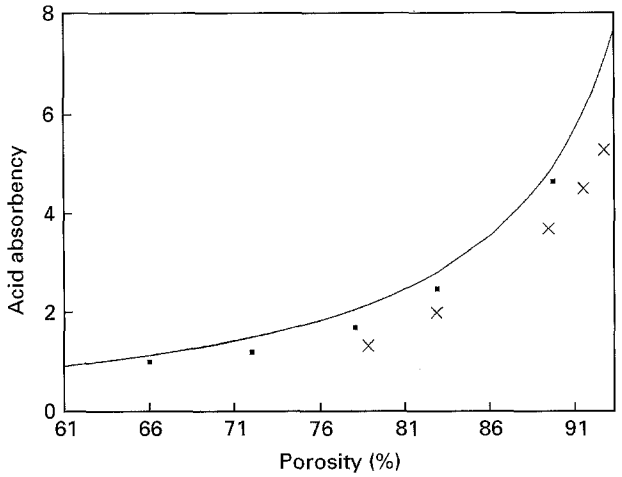

Figure 4 Acid absorbency versus porosity in the (×, ■) real and (—) theoretical matrices, obtained by (×) tape casting, and (■) rolling.

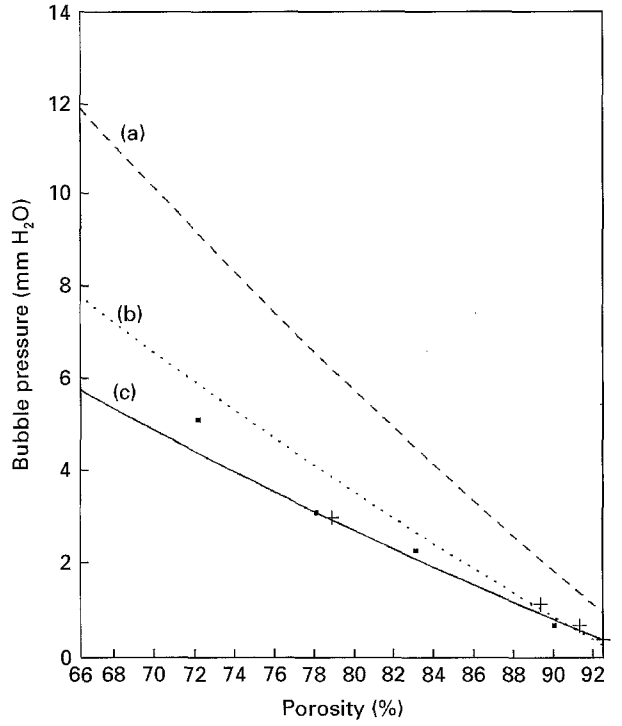

Figure 5 Bubble pressure versus porosity in the (+, ■) real and (---, ···, —) theoretical matrices having (a) 0.1 – 1 μm, (b) 1 – 10 μm, and (c) 10 – 50 μm pores, obtained by (+) tape casting, and (■) rolling.

Fig. 5 is a plot of bubble pressure versus porosity. The bubble pressure was calculated only for the cases of 0.1–1 μm, 1–10 μm and 10–50 μm, because the pores with length 0.01–0.1 μm may not have been retained, as discussed above. In this plot a scaling factor has been applied to obtain the theoretical curves. The upper values of bubble pressure were based on the assumption that gas exchange does not occur across the whole surface at the same time, and it must therefore be due to only one large pore. Thus in the case of pores of 10–50 μm in length, the calculated bubble pressure agreed with the real value.

A plot of current density is shown in Fig. 6. In the real matrix, differences between the rolling process

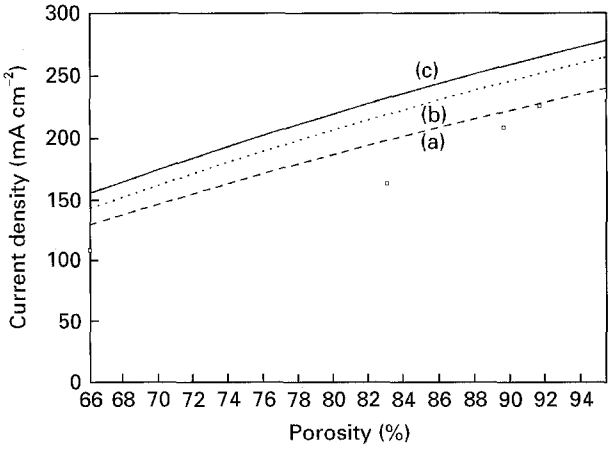

Figure 6 Current density versus porosity at 0.7 V in the (□) real and (—, ···, ---) theoretical matrices having (a) 0.1–1 μm, (b) 1 – 10 μm, and (c) 10 – 50 μm pores.

and the tape-casting process were not observed. The increase in theoretical current density with increasing porosity showed the same tendency as in the real values. The higher absolute values are due to the length of the ion conduction path, as mentioned above. The biggest difference was in the case of the pores 10–50 μm long. The roughness of the inner space in the matrix must be considered for accurate calculation.

4. Prediction of conditions needed for the best matrix

The results of the theoretical calculations show good correlation with the real matrix. We have attempted to calculate the best conditions of pore-size distribution, porosity, etc., in light of this modelling.

As shown in Fig. 5, a matrix with larger pores in the same porosity showed lower bubble pressures. It is known that a pressure above 500 mm H_2O is required for real use, and our results certified this fact. The matrices exhibiting a bubble pressure above 500 mm H_2O were chosen in all calculated cases. The values of porosity were 70% less for a matrix having pores 10–50 μm long, 75% less for a matrix having pores 1–10 μm long and 81% less for a matrix having pores 0.1–1 μm long. As shown in Fig. 6, the current density increased with increasing porosity. This result showed that the matrix with a 500 mm H_2O bubble pressure was best in certain pore-size distributions. The calculations were performed for all pore-size distributions on the basis of the above results. Fig. 7 shows the five types of pore-size distribution having the best performance with 20% of 0.01 – 0.1 μm pores (we assumed that these sizes of pore exist but do not affect properties); the porosity and current density are shown in Fig. 8. The matrix with small pores showed high porosity and high current density. Because only the small-sized pores have a limiting effect on increase in porosity, the best pore-size distribution consisted of 0.1–1 μm long pores, mainly with a small ratio of 1–10 μm pores for the porosity. The porosity was 80% in this case.

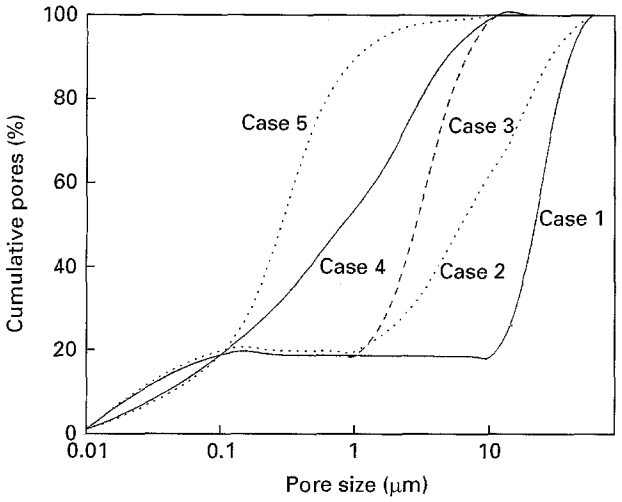

Figure 7 Pore-size distribution of the modelled matrix showing the best performance.

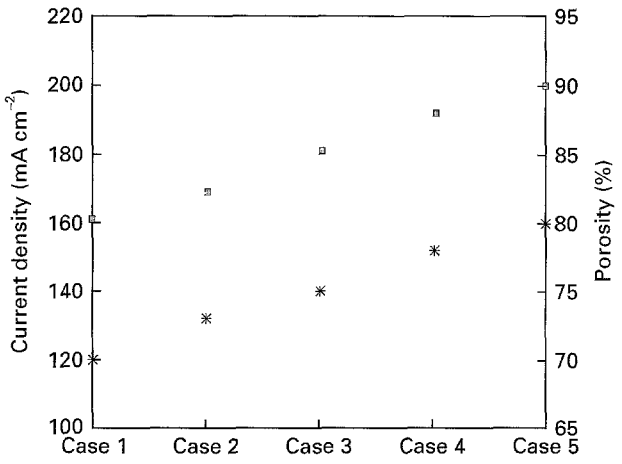

Figure 8 Relationship between (*) porosity and (□) current density at 0.7 V in the modelled matrix having the same bubble pressure.

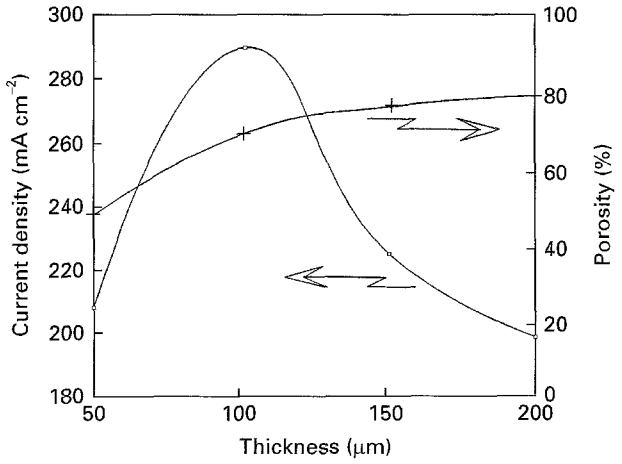

Figure 9 The variation of current density and porosity with thickness in the modelled matrix.

Fig. 9 shows a plot of porosity for the same bubble pressure and its current density at 0.7 V as a function of the thickness of the matrix using case 5 shown in Fig. 8. A decrease of thickness reduced the bubble pressure, and a decrease in porosity was required to maintain the same bubble pressure; the ion conduction path decreased with a decrease in the thickness. Eventually the current density reached a maximum at a thickness of 100 μm. In proportion to the decrease of thickness, the current density increased until 100 μm thickness, owing to the short ion path, but further decrease in the thickness reduced the current density due to the very low porosity [14].

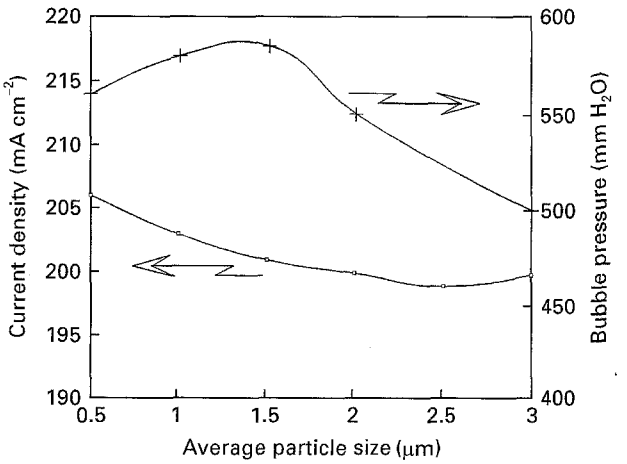

Figure 10 The variation of current density and bubble pressure with average particle size in the modelled matrix.

Fig. 10 shows the effect of particle size. In the case of 1.5 μm particle size, bubble pressure was maximum and the changes in current density were very small.

5. Conclusion

A comparison between theoretical and experimental values showed some errors in the model. First, pores below 0.1 μm existed and increased acid absorbency, but were not retained by phosphoric acid. Second, the effect of pore shape was neglected in calculations of bubble pressure and current density. Third, in the case of ions, interfacial properties like interfacial resistance, were neglected, and yielded high current density.

In spite of these errors, this model is successful in that the tendencies of the theoretical values were acquired. Prediction of the best conditions for making a real matrix could be possible through this simple model.

Acknowledgement

This work was supported by the Korea Institute of Energy Research.

References

1. A. McDOUGALL, (ed) in "Fuel Cells" (John Wiley & Sons, New York, 1976) pp. 5, 31.
2. A. ASCOLI, J. D. PANDYA and G. REDAELLI, *Energy* **14** (1989) 875.
3. A. J. APPLEBY and F. R. FOULKES, (eds) in "Fuel Cell Handbook" (Van Nostrand Reinhold, New York, 1989) p. 3.
4. J. M. FERET, *J. Power Sources*, **29** (1990) 59.

5. R. T. FOTEY, PhD thesis, University of Washington (1979).
6. J. C. TROCCIOLA, J. POWERS and R. G. MARTIN, US Pat. 4695 518 (1987).
7. R. D. BREAULT, US Pat. 4219 611 (1980).
8. K. H. YOON, H. I. LEE, K. H. LEE and C. S. KIM, *J. Kor. Ceram. Soc.* **29** (1992) 587.
9. K. H. YOON, J. H. HUH, J. H. JANG and C. S. KIM, *ibid.* **31** (1994) 375.
10. T. KATAN and H. F. BAUMAN, *J. Electrochem. Soc.* **122** (1975) 77.
11. C. E. BAUMGARTNER, *J. Am. Ceram. Soc.* **73** (1990) 516.
12. R. P. ICZKOWSKI, *J. Electrochem. Soc.* **111** (1964) 1078.
13. R. P. ICZKOWSKI and M. B. CULTLIP, *ibid.* **127** (1980) 1433.
14. C. LAGERGREN, G. LINDBERGH and D. SIMONSSON, *ibid.* **142** (1995) 787.

Received 6 September 1995
and accepted 8 May 1996